Proceedings of The Institute of Acoustics

A Pressure-Compensated Ring-Shell Projector

G. W. McMahon and B. A. Armstrong
Defence Research Establishment Atlantic

Introduction

Ring-shell underwater sound projectors have been under investigation at DREA for several years. A number of successful low frequency, high power sources have been built for operation at shallow depths. Essentially, the ring-shell projector comprises a piezoelectric ceramic ring sandwiched between two shallow spherical shell segments. Radial motion of the ring drives the shells in flexure with considerable enhancement of the volume velocity. A concave configuration of the shells has been used to achieve the best depth capability. However, in common with most low frequency projectors, the operating depth is still limited to a few tens of metres without some form of internal pressure compensation.

To address this problem, an experimental ring-shell projector has been built with an internal water bladder, open to the sea (Fig. 1). Ingress of water expands the bladder and compresses the internal air, supplying the necessary pressure compensation without seriously impeding the motion of the shells. A convex configuration of the shells is used to provide a greater internal air volume change and hence a greater depth range.

This paper describes the construction of the experimental projector and the finite element mathematical modelling that has been applied to it. Performance results, obtained at shallow depths, are compared to the finite element predictions, which are extended to cover the expected operating depth range. Finally, we present an outline of some potential design improvements that are indicated by our experience with this projector.

Construction

Figure 2 shows a cross section through one-half of the projector as it might appear when submerged to about 1/3 of its maximum operating depth. The piezoceramic ring comprises 56 staves of tangentially-poled lead zirconate titanate bonded with epoxy adhesive and connected electrically in parallel. The ring is given a compressive bias of about 20 MPa by an outer wrapping of fiberglass applied under tension and consolidated with epoxy resin. The aluminum shells are bonded and bolted to the ceramic ring. Fourteen narrow

aluminum staves are included in the ring to accommodate the bolts.

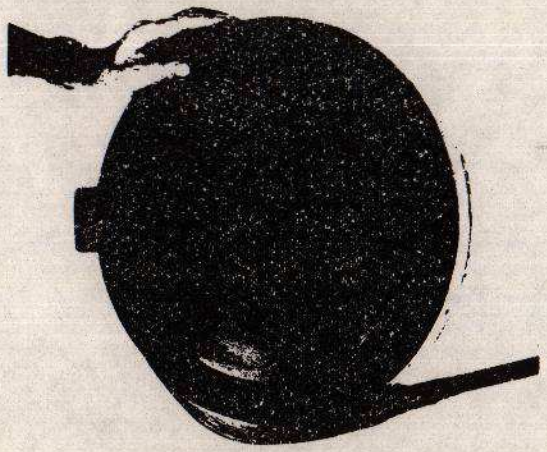

Fig. 1 Photograph of the pressure-compensated ring-shell projector.

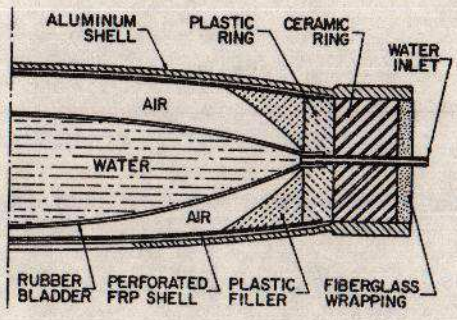

Fig. 2 Radial cross-section of the projector showing the water bladder partially filled.

The water bladder is made from two plane sheets of neoprene rubber whose edges are vulcanized together and encapsulated in a ring of plastic. The plastic ring is bonded to the ceramic ring; this process also encapsulates the electrical connections which are not shown. A stainless steel tube forms the water inlet. Shells of perforated fiberglass reinforced plastic (FRP) are attached to the plastic ring and spaced about 1.5 mm from the aluminum shells. These serve to support the weight of water in the bladder and prevent the bladder from touching the shells until it is nearly full of water. A flexible plastic filler is potted in the corners to increase the useful air volume compression ratio and prevent possible rupture of the bladder if the projector is lowered to excessive depths. Not shown in the diagram are an air valve which allows compressed air to be put into the projector and a tube to equalize the pressure in the two air cavities on opposite sides of the bladder. The air cavities can therefore be filled initially with one or two atmospheres of compressed air, which will more than double or triple the depth range compared to simple atmospheric pressure filling.

Finite Element Modelling

This projector was modelled by our finite element computer program named MAVART, an acronym representing mathematical Model for Analysis of the Vibrations and Acoustic Radiation of Transducers. It is capable of modelling the harmonic steady state response of a piezoelectrically driven body immersed in an infinite acoustic fluid. MAVART assumes infinite-fold axial symmetry but it can accurately model transducers having moderate deviations from this symmetry, such as our ring-shell projector, if appropriate material modifications are made.

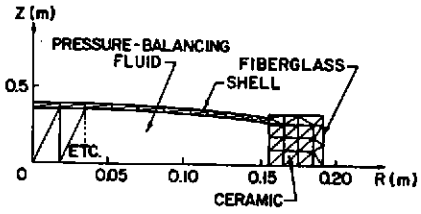

Fig. 3 MAVART finite element grid for the projector alone.

Figure 3 illustrates the finite element grid used to describe the ring-shell projector. In addition to the axial symmetry about the Z-axis, there is mirror symmetry in the Z=0 plane so only one quarter of the projector, with appropriate boundary conditions, needs to be modelled. To set up the model, the projector cross section is divided into a mesh of six-noded isoparametric triangles, each of which is a torus in a three-dimensional representation.

The fine geometrical details of the pressure balancing system were not modelled because the "wavelength" of the interior sound waves is much greater than the interior dimensions for frequencies less than 500 Hz. Rather, the depth compensating system was modelled as a fluid whose bulk modulus was altered to reflect the initial filling pressure and the pressure and volume changes due to depth. For simplicity, only a few of the internal fluid elements are drawn in Fig. 3.

The finite element grid for the projector immersed in an infinite fluid is illustrated in Fig. 4. A sphere of fluid, of radius sufficient to contain the projector, is divided in a similar manner as in Fig. 3. Only a portion of the fluid elements have been drawn and none of the solid elements, which have been shown in Fig. 3. On the surface of the fictitious fluid sphere the pressure and pressure gradient are matched to a spherical harmonic solution of the Helmholtz integral equation which represents the pressure in the external infinite fluid.

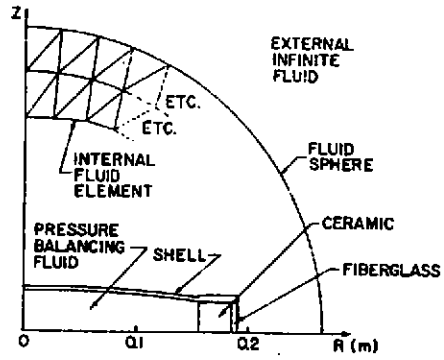

Fig. 4 Simplified finite element grid for the projector in an infinite acoustic medium.

The solution returned by MAVART comprises complex vector displacements at solid nodes and pressures at fluid nodes. At nodes with an electrical degree of freedom, the voltage is also returned. This solution is post-processed to give the far-field transmitting response, directivity patterns, electrical impedance and stresses and strains at solid nodes. The pressure at any point in the external medium can also be calculated.

Before modelling any transducer it is necessary to know the material properties of the components used in its construction. For the unwrapped ceramic ring the effective tangential material properties, which include the effects of the glue joints and aluminum staves, were determined from experimental measurements of the resonance and antiresonance frequencies and electrical capacitance. The material properties of the fiber-glass-epoxy wrapping were calculated from "book values" and were not refined with experimental results as the wrapping has little dynamic effect. "Book values" were also used for the aluminum shell. The effectiveness of this procedure can be judged from Table I. The first three values necessarily agree well as they were used to determine the material properties. The last five entries are testimony to the effectiveness of the method and the accuracy of MAVART.

TABLE I MEASURED AND COMPUTED RESONANCE FREQUENCIES AND CAPACITANCE

	Measured	MAVART
Ring alone in air; Resonance (Hz)	2644	2656
Antiresonance (Hz)	3210	3254
Capacitance (nF)	50.3	50.6
Projector in air; Fundamental (Hz)	800	790
Second shell resonance (Hz)	1337	1272
Third shell resonance (Hz)	2520	2529
Ring resonance (Hz)	3780	3852
Projector in water; Fundamental (Hz)	217	216

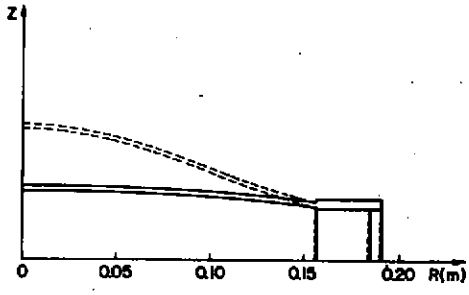

Fig. 5 Diagram showing the form of the displacement at resonance as computed by MAVART.

Figure 5 is an exaggerated plot of the displacement of the solid nodes at 211 Hz, the resonance frequency at a shallow depth. When the ceramic ring displaces radially, the centre of the shell displaces 50 times as far in an axial direction. For a 3500-volt rms driving voltage, the peak-to-peak displacement is 2.5 mm. Pressure amplitude contours produced by this displacement are shown in Fig. 6. It is apparent that, along the Z-axis at a radius close to 25 cm, the wavefront is circular.

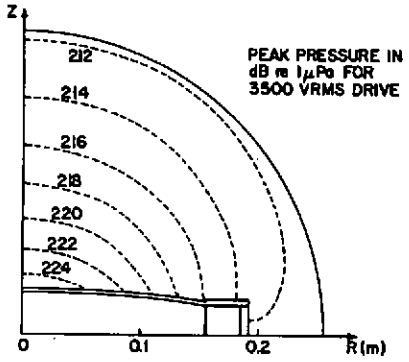

Fig. 6 Contours of peak pressure amplitude computed by MAVART in the near field of the projector for a 3500 V drive at resonance.

MAVART analysis shows that the far-field pressure may be measured at a test distance of 50 cm with a correction of only 0.15 dB subtracted from the measured pressure. This correction is practically independent of frequency up to 400 Hz.

Results and Discussion

Performance testing was carried out on the ring-shell projector in sea water at depths to 35 metres, the maximum available at the calibration facility. Transmitting responses were measured using a test distance of 50 cm so that interfering reflections from boundaries were small. A typical transmitting response curve is shown in Fig. 7 over the frequency range 150 to 500 Hz. The points are the experimental results and the curve is computed by MAVART. The initial filling pressure for these results was 2 atmospheres absolute and the depth was 20 metres.

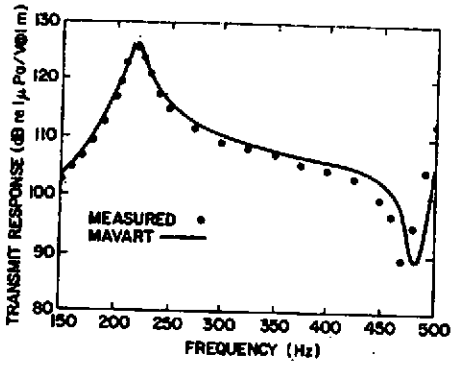

Fig. 7 Measured and computed transmitting responses of the projector at 20 m depth with a fill pressure of 2 atm.

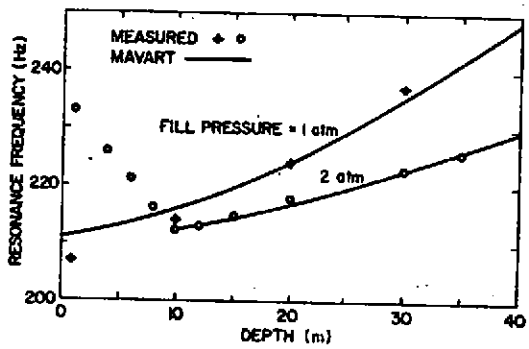

Fig. 8 Measured and computed resonance frequencies as functions of depth for two fill pressures.

The resonance frequency in water increases somewhat with depth due to the decreasing compliance of the internal air. Tests were carried out with initial fill pressures of 1, 1.5 and 2 atm absolute. Figure 8 shows graphs of resonance frequency vs depth for 1 and 2 atm initial pressure. The points are experimental measurements and the lines are MAVART predictions. The frequency increases for depths less than the initial internal pressure depth as seen by the measured results below 10 metres for 2 atm pressure. This is because the shell curvature is increased by the excess internal pressure. At 10 metres depth the internal and external pressures become equal and compression of the internal air begins. No significant change in the level of the peak transmitting response was noted at any fill pressure or depth.

In Fig. 9, the MAVART results of Fig. 8 are extended to greater depths than were available for experimental measurements and a curve for 4 atm initial pressure is included. The curves begin at the depth where the water bladder just begins to fill and terminate (for 1 and 2 atm) at the estimated maximum operating depth where the bladder touches the shells. This corresponds to an air volume compression ratio of 8 to 1 determined from pressure tank measurements. MAVART predicts that the peak transmitting response is lowered less than 1 dB up to 150 metres depth (2 atm fill pressure). The experimental

projector would not likely be strong enough to withstand a fill pressure of 4 atm at the surface but the compressed air could be introduced after reaching 30 metres depth. Note that an air pressure control system would allow this projector to be tuned from 238 to 300 Hz at a depth of 70 metres. On the other hand, the resonance frequency of a projector having thicker stiffer shells would depend less on depth.

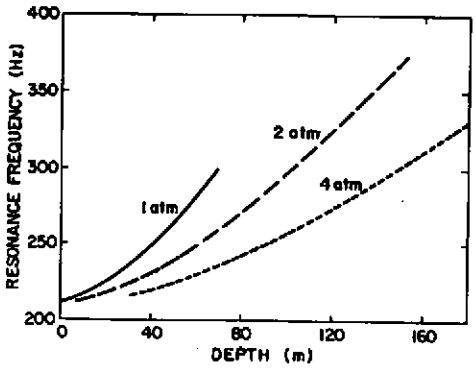

Fig. 9 Resonance frequency as functions of depth computed by MAVART for three fill pressures.

The measured electroacoustic efficiency at resonance ranges from 70 to 80%, somewhat lower than has been observed for ring-shell projectors without pressure compensation. The efficiency remains greater than 50% between the -10 dB points, a band of about 55 Hz. Extra losses can be attributed to the plastic filler of flexible polyurethane and viscous losses in the air between the aluminum and FRP shells.

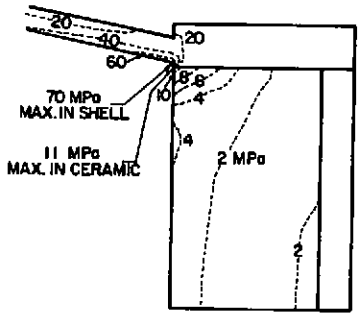

Fig. 10 Peak principal dynamic stress contours in the ceramic ring and adjacent shell for 3500 V drive at resonance. For clarity, the vertical scale has been expanded.

The maximum source level from this projector is estimated at 197 dB re 1 μPa at 1 m or about 400 watts. This corresponds to a driving voltage of 3500 volts rms and a field of 2 kV/cm in the ceramic ring. The peak dynamic stresses in the ring and aluminum shells were analyzed by MAVART and are shown in Fig. 10 as principal stress contours for the maximum drive voltage of 3500 V rms. These stress levels, both mechanical and electrical, are reasonable if not conservative. Note that the point of maximum stress in the ceramic is at the corner where it joins the flange of the shell. MAVART analysis has shown that this stress can be reduced considerably by increasing the flange

depth at this point.

Potential Design Improvements

The experimental ring-shell projector was designed to achieve the lowest practical resonance frequency in such a small size. Consequently its resonance frequency has a pronounced dependence on depth. To reduce this dependence and maintain the same resonance requires proportionately thicker stiffer shells in a projector of larger size. Bandwidth would also increase due to the increased radiation resistance and the source level would rise.

The projector can be made much more robust with little sacrifice of performance. Dynamic stress in the ceramic is likely to be the factor that limits source level and increasing the inner flange thickness sharply reduces the stress. A combination of thicker shells, thicker shell flange and more aluminum staves and bolts would allow higher initial filling pressure and hence greater depth range.

The electroacoustic efficiency may be improved by redesign of the internal support structure for the water bladder (FRP shells) and by careful selection of low loss plastic materials for the interior potting. The support structure, for example, could be a framework of light rods or wires to eliminate the somewhat confined layers of air that presently exist between the aluminum shells and the FRP shells.

Conclusions

The operating depth range of a ring-shell projector has been extended by using an internal water bladder for pressure compensation. The depth range may be further extended by pre-filling the projector with compressed air.

The resonance frequency increases with depth due to the decreasing compliance of the internal air but the transmitting response about the resonance is nearly independent of depth. The efficiency is over 70% at resonance and remains greater than 50% between the -10 dB points.

Experience with the first experimental projector has identified a number of areas where the design can be improved.